Physics Letters B 677 (2009) 54–58

Contents lists available at ScienceDirect

Physics Letters B

www.elsevier.com/locate/physletb

Impact on the light Higgsino-LSP scenario from physics beyond the minimal supersymmetric standard model

Kingman Cheung [a,b,c], Seong Youl Choi [d], Jeonghyeon Song [c,e,*]

[a] Dept. of Physics, National Tsing Hua University, Hsinchu, Taiwan
[b] Physics Division, National Center for Theoretical Sciences, Hsinchu, Taiwan
[c] Division of Quantum Phases & Devices, School of Physics, Konkuk University, Seoul 143-701, Republic of Korea
[d] Dept. of Physics and RIPC, Chonkuk National University, Jeonju 561-756, Republic of Korea
[e] Dept. of Physics, University of Wisconsin, Madison, WI 53706, USA

ARTICLE INFO

Article history:
Received 1 April 2009
Received in revised form 1 May 2009
Accepted 8 May 2009
Available online 15 May 2009
Editor: M. Cvetič

PACS:
12.60.Jv
14.80.Bn
14.80.Ly

ABSTRACT

The modest addition of the dimension-5 term $\lambda(\hat{H}_u \cdot \hat{H}_d)^2/M$ to the superpotential of the minimal supersymmetric standard model (MSSM) originated from physics beyond the MSSM (BMSSM) has a significant impact on the scenario of the Higgsino-dominated neutralino state being the lightest supersymmetric particle (LSP). It increases the mass difference between the LSP and the lighter chargino as well as that between the LSP and the second-lightest neutralino. This enhances the LHC discovery potential of the chargino and neutralino decays, producing more energetic charged leptons or pions than the decays without the BMSSM corrections. Furthermore, the coannihilation between the lighter chargino or second-lightest neutralino and the LSP is reduced substantially such that the LSP mass does not have to be very heavy. Consequently, an almost pure Higgsino LSP with its mass ~ 100 GeV in the BMSSM can account for all the relic density of cold dark matter in the Universe unless $\tan\beta$ is too large.

1. Introduction

The presence of cold dark matter (CDM) in our Universe is now well established by the very precise measurement of the cosmic microwave background radiation in the Wilkinson Microwave Anisotropy Probe (WMAP) experiment [1]. A nominal 3σ range of the CDM relic density is

$$\Omega_{\rm CDM}h^2 = 0.105^{+0.021}_{-0.030}, \tag{1}$$

where h is the Hubble constant in units of 100 km/Mpc/s.

One of the most appealing and natural CDM particle candidates is provided by supersymmetric models with R-parity conservation [2]. This R-parity conservation ensures the stability of the lightest supersymmetric particle (LSP) so that the LSP can be CDM. The LSP is in general the lightest neutralino, a linear combination of neutral electroweak (EW) gauginos and Higgsinos. Since the LSP nature depends on its compositions, its detection can vary a lot.

An interesting scenario is the Higgsino-like LSP, which can arise from a number of supersymmetry breaking models, e.g., focus-point supersymmetry models [3] or whenever the μ parameter is much smaller than the Bino and Wino masses [4]. In the minimal supersymmetric standard model (MSSM) [5], the Higgsino-LSP scenario implies nearly-degenerate Higgsino states: Coannihilation is too efficient so that the observed CDM relic density requires a rather heavy Higgsino state with mass around 1–1.2 TeV [6]. Moreover, the mass degeneracies between the LSP ($\tilde{\chi}_1^0$) and the lighter chargino/second-lightest neutralino ($\tilde{\chi}_1^\pm/\tilde{\chi}_2^0$) generate too soft decay products for detecting the states $\tilde{\chi}_1^\pm$ and $\tilde{\chi}_2^0$ at the LHC. Thus, the Higgsino-LSP in the MSSM posts a difficult scenario at the LHC.

In this Letter we show that the modest addition of a dimension-5 term $\lambda(\hat{H}_u \cdot \hat{H}_d)^2/M$ to the MSSM superpotential, a scenario beyond MSSM (BMSSM) [7], alleviates the difficulties of the Higgsino-LSP scenario. It has been discussed that non-renormalizable and high-dimensional operators in new physics models can yield important consequences in low energy phenomenology [8,9]. As shall be demonstrated in the following, this dimension-5 term, $\lambda(\hat{H}_u \cdot \hat{H}_d)^2/M$, lifts up the degeneracy between the states $\tilde{\chi}_1^0$ and $\tilde{\chi}_1^\pm/\tilde{\chi}_2^0$ [10], thus enhancing the discovery potential of the chargino and neutralino decays with more energetic charged leptons or pions than the decays in the MSSM. In addition, the coannihilation of the LSP with $\tilde{\chi}_1^\pm$ or $\tilde{\chi}_2^0$ is reduced substantially such that a light Higgsino-LSP with a mass around 100 GeV can accommodate the WMAP data on the CDM relic density.

* Corresponding author at: Division of Quantum Phases & Devices, School of Physics, Konkuk University, Seoul 143-701, Republic of Korea.
E-mail address: jhsong@konkuk.ac.kr (J. Song).

0370-2693 © 2009 Elsevier B.V. Open access under CC BY license.
doi:10.1016/j.physletb.2009.05.022

2. BMSSM

Albeit many virtues of low energy supersymmetry (SUSY), fine-tuning in the lightest Higgs boson mass m_h motivates additional degrees of freedom to the MSSM [10]. New interactions beyond the MSSM at the TeV scale M may be encoded in higher-dimensional operators. Recently, Dine et al. [7] have shown that the most general dimension-5 superpotential term for the MSSM Higgs sector is

$$W_{\text{dim-5}} = \frac{\lambda}{M}(\hat{H}_u \cdot \hat{H}_d)^2, \tag{2}$$

with the SU(2) contraction $\hat{H}_u \cdot \hat{H}_d = \hat{H}_u^+ \hat{H}_d^- - \hat{H}_u^0 \hat{H}_d^0$ for the up-type and down-type Higgs doublet superfields, $\hat{H}_u$ and $\hat{H}_d$, respectively. This dimension-5 operator has been shown to raise easily the lightest Higgs boson mass above the LEP bound without loss of naturalness [11].

Another dimension-5 operator, which breaks SUSY and affects the Higgs spectrum, is

$$\int d^2\theta\, \mathcal{Z}\frac{\lambda}{M}(\hat{H}_u \cdot \hat{H}_d)^2, \tag{3}$$

where $\mathcal{Z} = \theta^2 m_{\text{SUSY}}$ is the spurion field with the SUSY breaking scale m_{SUSY} [7]. If $m_{\text{SUSY}} \simeq |\mu|$, the correction to m_h comes dominantly from the supersymmetric operator in Eq. (2) rather than that in Eq. (3). The correction is given to leading order in the dimensionless parameter $\varepsilon \equiv \lambda\mu/M$ by

$$\begin{aligned}\delta m_h^2 &= \varepsilon v^2\left[1 + 2s_{2\beta} + \frac{2(m_A^2 + m_Z^2)s_{2\beta}}{\sqrt{(m_A^2 - m_Z^2)^2 + 4m_A^2 m_Z^2 s_{2\beta}^2}}\right] \\ &\simeq 8\frac{m_A^2}{m_A^2 - m_Z^2}v^2\frac{\varepsilon}{\tan\beta} + \mathcal{O}\left(\frac{\varepsilon}{\tan^2\beta}\right),\end{aligned} \tag{4}$$

where $v \approx 246$ GeV is the Higgs vacuum expectation value and the second expression holds for large $\tan\beta$. For simplicity we take the CP-conserving framework and decoupling limit of $m_A \gg m_Z$ in the following. Note that the BMSSM correction is inversely proportional to $\tan\beta$ in contrast to the conventional radiative corrections. The correction δm_h normalized by m_h around the LEP bound is roughly $\delta m_h/m_h \simeq 20\varepsilon/\tan\beta$ for $m_A \gg m_Z$. For $\varepsilon = 0.05$ the correction can be as large as 50% (10%) for $\tan\beta = 2$ (10). Therefore, the LEP bound is easily satisfied by a *positive* $\varepsilon \sim 0.1$.

The interaction terms that involve only the Higgsino fields ($\tilde{H}_{u,d}$) and Higgs fields ($H_{u,d}$) are given by

$$\begin{aligned}\mathcal{L}_H = &-\mu(\tilde{H}_u \cdot \tilde{H}_d) - \frac{\lambda}{M}\big[2(H_u \cdot H_d)(\tilde{H}_u \cdot \tilde{H}_d) \\ &+ 2(H_u \cdot \tilde{H}_d)(\tilde{H}_u \cdot H_d) + (\tilde{H}_u \cdot H_d)^2 + (H_u \cdot \tilde{H}_d)^2\big] + \text{H.c.}\end{aligned} \tag{5}$$

After EW symmetry and SUSY breaking, the modified neutralino mass matrix $\mathcal{M}_N$ in the $\{\tilde{B}, \tilde{W}^3, \tilde{H}_d^0, \tilde{H}_u^0\}$ basis reads:

$$\mathcal{M}_N = \begin{pmatrix} M_1 & 0 & -m_Z s_W c_\beta & m_Z s_W s_\beta \\ 0 & M_2 & m_Z c_W c_\beta & -m_Z c_W s_\beta \\ -m_Z s_W c_\beta & m_Z c_W c_\beta & \frac{\lambda}{M}v^2 s_\beta^2 & -\mu + \frac{2\lambda}{M}v^2 c_\beta s_\beta \\ m_Z s_W s_\beta & -m_Z c_W s_\beta & -\mu + \frac{2\lambda}{M}v^2 c_\beta s_\beta & \frac{\lambda}{M}v^2 c_\beta^2 \end{pmatrix}, \tag{6}$$

and the modified chargino mass matrix $\mathcal{M}_C$ in the $\{\tilde{W}^-, \tilde{H}^-\}$ basis reads:

$$\mathcal{M}_C = \begin{pmatrix} M_2 & \sqrt{2}m_W s_\beta \\ \sqrt{2}m_W c_\beta & \mu - \frac{\lambda}{M}v^2 c_\beta s_\beta \end{pmatrix}, \tag{7}$$

where $s_\beta = \sin\beta$, $s_W = \sin\theta_W$, etc. To leading order in ε, the BMSSM effects on the masses of $\tilde{\chi}_1^0$, $\tilde{\chi}_2^0$, and $\tilde{\chi}_1^\pm$ are, in the light Higgsino case ($M_{1,2} \gg m_Z, \mu$), [12]

$$\begin{aligned} m_{\tilde{\chi}_{1,2}^0} &\simeq |\mu|\left[1 - \frac{v^2}{2\mu^2}(2s_{2\beta} \pm 1)\varepsilon\right] \\ &\quad + \text{sign}(\mu)\frac{(M_1 c_W^2 + M_2 s_W^2)m_Z^2}{2M_1 M_2}(1 \pm s_{2\beta}), \\ m_{\tilde{\chi}_1^\pm} &\simeq |\mu|\left[1 - \frac{v^2}{2\mu^2}s_{2\beta}\varepsilon\right] - \text{sign}(\mu)\frac{m_W^2 s_{2\beta}}{M_2}, \end{aligned} \tag{8}$$

where in the first equation the upper (lower) sign is for $\tilde{\chi}_1^0$ ($\tilde{\chi}_2^0$) mass. With increasing ε both the $\tilde{\chi}_1^0$ and $\tilde{\chi}_1^\pm$ masses decrease; the $\tilde{\chi}_2^0$ mass increases for large $\tan\beta \gtrsim 4$ but decreases for small $\tan\beta \lesssim 4$, if the $m_W/M_{1,2}$ correction is ignored. However, since the LSP mass drops faster than the $\tilde{\chi}_1^\pm$ mass with increasing ε, sizable mass differences between $\tilde{\chi}_1^\pm$ and $\tilde{\chi}_1^0$ as well as between $\tilde{\chi}_2^0$ and $\tilde{\chi}_1^0$ are developed. Due to the decreasing mass of $\tilde{\chi}_1^\pm$ with ε, the lower mass bound of $m_{\tilde{\chi}_1^\pm} \gtrsim 94$ GeV [13] can constrain the BMSSM light Higgsino-LSP scenario. If μ is negative, the second term in the expressions of $m_{\tilde{\chi}_1^\pm}$ in Eq. (8) slows down the lighter chargino mass, which leads to larger mass difference between $\tilde{\chi}_1^0$ and $\tilde{\chi}_1^\pm$. Therefore, the negative μ case accommodates larger parameter space to explain all the WMAP data by the Higgsino-LSP. However we note that the combined analysis for the anomalous magnetic moment of the muon as well as $b \to s\gamma$ prefers a positive μ [14]. In what follows, therefore, we take the case of positive μ.

3. Collider detection

It is well known [12] that in the Higgsino-LSP scenario the mass degeneracy among $\tilde{\chi}_1^0$, $\tilde{\chi}_2^0$, and $\tilde{\chi}_1^\pm$ renders their detection at colliders extremely difficult, even though radiative corrections can increase the mass difference by a few GeV [15].[1] The decay products of $\tilde{\chi}_1^\pm$ or $\tilde{\chi}_2^0$ are too soft for their detection. In the BMSSM, the new contribution from the dimension-5 term in Eq. (2) can alleviate the Higgsino-LSP detection problem significantly by inducing sizable mass splittings between $\tilde{\chi}_1^0$ and $\tilde{\chi}_1^\pm/\tilde{\chi}_2^0$. On the other hand, the Higgsino fraction of the LSP remains high enough to call the LSP a pure Higgsino as long as the gaugino masses are large. The effect of ε on the neutralino mixing matrix N, which diagonalizes the neutralino mass matrix as $N^* \mathcal{M}_N N^\dagger = \text{diag}(m_{\tilde{\chi}_1^0}, \ldots, m_{\tilde{\chi}_4^0})$, corresponds to the rotation of $\tilde{H}_d^0$ and $\tilde{H}_u^0$ components. Therefore the LSP Higgsino fraction, $P_{\tilde{H}} = |N_{13}|^2 + |N_{14}|^2$, remains intact by the change of the ε parameter. In the limit of large gaugino masses, we have almost pure Higgsino LSP since $P_{\tilde{H}} \simeq 1 - \mathcal{O}(m_W/M_1)$.

In Fig. 1, we show the mass splittings, $\Delta m_0 \equiv m_{\tilde{\chi}_2^0} - m_{\tilde{\chi}_1^0}$ and $\Delta m_\pm \equiv m_{\tilde{\chi}_1^\pm} - m_{\tilde{\chi}_1^0}$, due to the BMSSM corrections as a function of ε for a specific choice of parameters: $M_2 = 2M_1 = 1$ TeV, $\mu = 120$ GeV and $\tan\beta = 3$. In this parameter set, the LSP mass is 70–110 GeV. For $\varepsilon = 0.05$–0.1, the mass difference between $\tilde{\chi}_1^\pm$ and $\tilde{\chi}_1^0$ is about 15–30 GeV and the mass difference between $\tilde{\chi}_2^0$ and $\tilde{\chi}_1^0$ is about 15–40 GeV. These mass splittings are much larger than those due to radiative corrections, which are typically a few GeV. Such sizable mass differences can help us detect the lighter chargino or second-lightest neutralino by tagging more energetic charged leptons or jets in the decay products. Consequently, the phenomenological impact of the BMSSM corrections on the SUSY search at the LHC is expected significant. Nevertheless, we do not perform any full-fledged analysis in the present work, expecting that such a comprehensive analysis will lead to almost the same physical conclusions as those described above.

[1] The radiative corrections to the mass splittings can be as large as 10 GeV if the stop mixing angle and mass splitting are large. See Ref. [16].

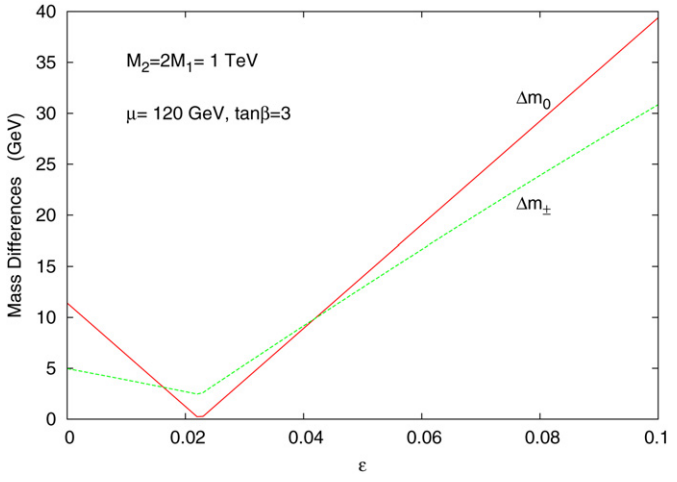

Fig. 1. The mass difference $\Delta m_0 = m_{\tilde{\chi}_2^0} - m_{\tilde{\chi}_1^0}$ (solid) between the second lightest neutralino and the LSP and the mass difference $\Delta m_\pm = m_{\tilde{\chi}_1^\pm} - m_{\tilde{\chi}_1^0}$ (dashed) between the lighter chargino and the LSP as a function of the BMSSM correction parameter ε.

4. Dark matter

In the MSSM Higgsino-LSP scenario, the strong coannihilation due to mass degeneracy pushes the Higgsino mass rather high, about 1–1.2 TeV, to account for the CDM relic density in Eq. (1). We note, in passing, that the MSSM radiative corrections affect the relic density rather mildly [17]. In the BMSSM, however, the large mass differences of Δm_0 and $\Delta m_\pm$ can suppress the coannihilation effectively; a much lighter Higgsino-LSP can account for the CDM relic density.

Another compelling feature in the BMSSM arises from the modified $\tilde{\chi}_1^0$–$\tilde{\chi}_1^0$–Z coupling which is proportional to $(|N_{13}|^2 - |N_{14}|^2)$. The ε dependence can be easily seen from the first row of the matrix to leading order in the BMSSM corrections, as

$$N_{1i} \sim \left(0, 0, \frac{1+\varepsilon_h}{\sqrt{2}}, \frac{1-\varepsilon_h}{\sqrt{2}}\right), \tag{9}$$

where $\varepsilon_h = \varepsilon v^2 c_{2\beta}/(4\mu^2)$, and we ignore small terms of $\mathcal{O}(m_W/M_1)$ as well as an overall phase [18]. In the MSSM ($\varepsilon = 0$), the light Higgsino-LSP scenario implies an almost vanishing $\tilde{\chi}_1^0$–$\tilde{\chi}_1^0$–Z vertex. In the BMSSM, the modified neutralino mixing matrix N in Eq. (9) leads to a sizable $\tilde{\chi}_1^0$–$\tilde{\chi}_1^0$–Z vertex, linearly proportional to ε. Therefore, the annihilation process $\tilde{\chi}_1^0\tilde{\chi}_1^0 \to Z \to f\bar{f}$ can be enhanced by the BMSSM corrections, giving a profound effect on the relic density of the LSP.

For a simple quantitative estimate we use a useful formula for the CDM relic density [2]

$$\Omega_{\tilde{H}} h^2 \approx \frac{0.1 \text{ pb}}{\langle \sigma_{\text{eff}} v \rangle}. \tag{10}$$

We include all the $2 \to 2$ self-annihilation and coannihilation processes in calculating the effective annihilation cross section σ_{eff}. Since the mass difference Δm_0 is substantially larger than $\Delta m_\pm$ for $\varepsilon \sim 0.1$ (see Fig. 1), we ignore the $\tilde{\chi}_1^0\tilde{\chi}_2^0$ coannihilation in estimating $\langle \sigma_{\text{eff}} v \rangle$ and use the following formula for a crude estimate of the thermally-averaged effective annihilation cross section, taking into account the coannihilation from $\tilde{\chi}_1^\pm$:

$$\langle \sigma_{\text{eff}} v \rangle = \frac{\sigma_{\tilde{\chi}_1^0\tilde{\chi}_1^0} v_{\tilde{\chi}_1^0\tilde{\chi}_1^0} + 2\sigma_{\tilde{\chi}_1^0\tilde{\chi}_1^\pm} v_{\tilde{\chi}_1^0\tilde{\chi}_1^\pm} (1 + \frac{\Delta m_\pm}{m_{\tilde{\chi}_1^0}})^{3/2} e^{-\Delta m_\pm/T_f}}{[1 + 2(1 + \frac{\Delta m_\pm}{m_{\tilde{\chi}_1^0}})^{3/2} e^{-\Delta m_\pm/T_f}]^2}. \tag{11}$$

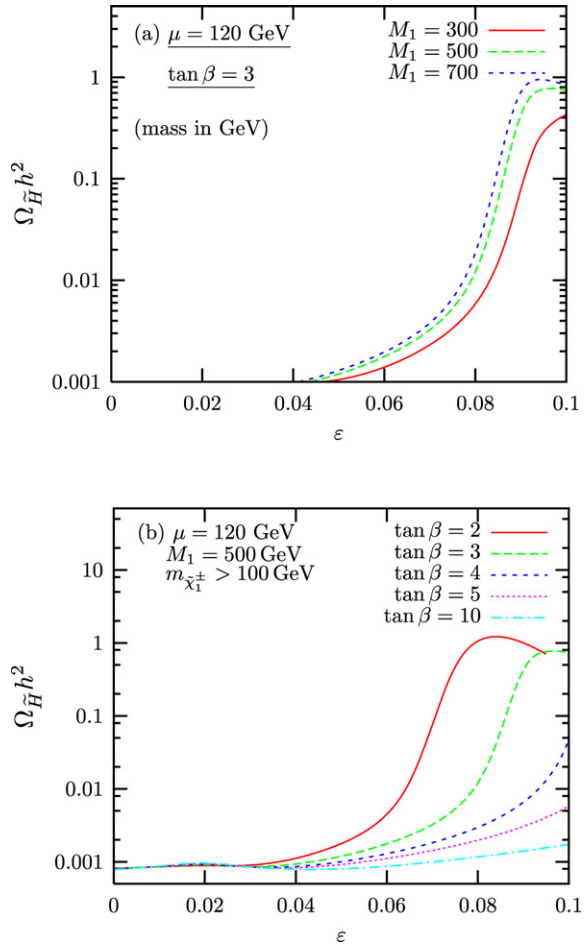

Fig. 2. The Higgsino-LSP relic density $\Omega_{\tilde{H}} h^2$ as a function of ε: (a) for the fixed $\tan\beta = 3$ with $M_1 = 300, 550, 700$ GeV, and (b) for the fixed $M_1 = M_2/2 = 300$ GeV with $\tan\beta = 2, 3, 4, 5, 10$. We set $\mu = 120$ GeV and other SUSY mass parameters to 1 TeV.

We take the freeze-out temperature $T_f = m_{\tilde{\chi}_1^0}/25$ and the relative velocity $v_{ij} = 0.3$ during the freeze-out. For the self-annihilation cross section ($\sigma_{\tilde{\chi}_1^0\tilde{\chi}_1^0}$) we consider the processes $\tilde{\chi}_1^0\tilde{\chi}_1^0 \to hh, Z^0h, Z^0Z^0, W^+W^-, f\bar{f}$. For the coannihilation cross section ($\sigma_{\tilde{\chi}_1^0\tilde{\chi}_1^-}$) we include the processes $\tilde{\chi}_1^0\tilde{\chi}_1^- \to W^-h^0, W^-Z^0, W^-\gamma, f\bar{f}'$ [19]. In the following numerical analysis we fix $m_{\tilde{Q}_L} = m_{\tilde{q}_R} = m_{\tilde{l}} = -A = m_A = 1$ TeV and include all the radiative corrections to the masses of neutralinos, charginos, and the Higgs bosons.

In Fig. 2, we show the $\tan\beta$- and M_1-dependence of the relic density $\Omega_{\tilde{H}} h^2$ versus ε with the fixed $\mu = 120$ GeV. In Fig. 2(a), we fix $\tan\beta = 3$ and take three typical values of $M_1 = 300, 500, 700$ GeV. As expected, the relic density increases with ε due to the suppressed coannihilation. In addition, we observe that decreasing M_1 reduces the LSP relic density. This is because the effective annihilation cross section σ_{eff}, dominated by the process $\tilde{\chi}_1^0\tilde{\chi}_1^0 \to f\bar{f}$ for sizable ε, is enhanced by the stronger Bino–Higgsino mixing for smaller M_1. Nevertheless the M_1-dependence of the relic density is rather mild.

On the other hand, the $\tan\beta$-dependence of $\Omega_{\tilde{H}} h^2$ is strong, as can be seen from Fig. 2(b). We take $\tan\beta = 2, 3, 4, 5, 10$ for the fixed $\mu = 120$ GeV and $M_1 = 500$ GeV. The $\tan\beta = 2$ case has the curve terminated at a large ε as $m_{\tilde{\chi}_1^\pm}$ gets below the experimental bound, $m_{\tilde{\chi}_1^\pm} > 100$ GeV. Up to $\varepsilon \approx 0.08$, the relic density is increasing with ε, because of more suppressed coannihilation. And $\Omega_{\tilde{H}}$ is larger for smaller $\tan\beta$, which can be attributed to

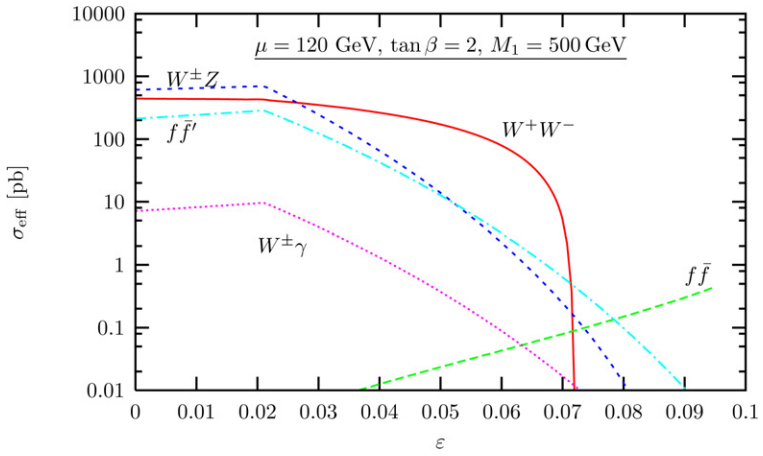

Fig. 3. The effective self and coannihilation cross sections. The W^+W^- mode is from the $\tilde{\chi}_1^0\tilde{\chi}_1^0$ self-annihilation while the $W^\pm Z/W^\pm\gamma$ modes from the $\tilde{\chi}_1^0\tilde{\chi}_1^\pm$ coannihilation.

the $\tan\beta$-dependence of the masses in Eq. (8): Small $\tan\beta \simeq 1$ maximally reduces the LSP mass, and thus enhances the mass difference $\Delta m_\pm$, suppressing the coannihilation. The slope of increasing $\Omega_{\tilde{H}}$ around $\varepsilon \simeq 0.08$ is very steep, due to the kinematic closure of $\tilde{\chi}_1^0\tilde{\chi}_1^0 \to W^+W^-$ mode ($m_{\tilde{\chi}_1^0}$ is decreasing). Another interesting feature is that after $\varepsilon \approx 0.08$ the relic density in the small $\tan\beta$ case turns its direction and decreases. This is because, as ε increases, the $\tilde{\chi}_1^0$–$\tilde{\chi}_1^0$–Z vertex becomes stronger and thus the self-annihilation process $\tilde{\chi}_1^0\tilde{\chi}_1^0 \to Z \to f\bar{f}$ is enhanced. Finally we observed that the WMAP data of $\Omega_{\tilde{H}}h^2 \simeq 0.1$ with positive μ strongly prefer small $\tan\beta$. If $\tan\beta \gtrsim 4$, the WMAP data can be only partially explained. Of course, if μ is negative, a much larger parameter space is allowed for the WMAP data.

In order to understand the behavior of the relic density against ε (especially for the bumpy shape), we calculate the contribution of each channel for small $\tan\beta = 2$ case. Fig. 3 shows the *effective* annihilation cross section $\sigma_{\rm eff}$ as a function of ε. Here we set $\mu = 120$ GeV, and $M_1 = 500$ GeV. We take into account the thermal suppression factor due to the mass difference. The effective $\tilde{\chi}_1^0\tilde{\chi}_1^\pm$ coannihilation cross section is defined by $\sigma_{\rm eff}[\tilde{\chi}_1^0\tilde{\chi}_1^\pm] = 2\sigma_{\tilde{\chi}_1^0\tilde{\chi}_1^\pm}(1+\Delta m_\pm/m_{\tilde{\chi}_1^0})^{3/2}e^{-\Delta m_\pm/T_f}$. For the $\tilde{\chi}_1^0\tilde{\chi}_1^0$ self-annihilation, the W^+W^- and $f\bar{f}$ modes are the dominant channels. As ε increases, the LSP mass $m_{\tilde{\chi}_1^0}$ decreases. For $\varepsilon \gtrsim 0.072$ the W^+W^- mode is kinematically closed. The self-annihilation process $\tilde{\chi}_1^0\tilde{\chi}_1^0 \to f\bar{f}$ is enhanced due to the $\tilde{\chi}_1^0$–$\tilde{\chi}_1^0$–Z vertex being stronger with increasing ε. On the other hand, the coannihilation channels, dominant for small ε, become suppressed with larger ε due to larger mass splittings. As a whole, we have the bump-shaped distribution of the relic density as a function of ε in Fig. 2(b). One technical issue can arise when we calculate the thermally averaged annihilation cross section near W^+W^- thresholds. Since we fix the relative velocity, there is some discrepancy in the cross section which is sensitive to the actual relative velocities near the threshold. A more detailed analysis based on the exact Boltzmann equation will be required for more accurate estimates of the cross sections, which is, however, beyond the scope of the present short report.

Another important experimental test for the Higgsino-LSP scenario is the spin-independent scattering cross section $\sigma_{\chi p}^{\rm SI}$ of the LSP with nucleons. We have calculated the scattering cross section $\sigma_{\chi p}^{\rm SI}$ based on the input parameters given in Ref. [20]. As shown in Fig. 4, if ε is larger than 0.02, the elastic scattering cross section $\sigma_{\chi p}^{\rm SI}$ is reduced far below the current limits, mainly because the lightest Higgs boson mass m_h increases with the BMSSM corrections. Here we briefly comment on the spin-dependent scattering cross sections. The spin-dependent scattering process, which is experimentally more difficult to extract because of the lack of coherent enhancement unlike the spin-independent process, is mainly mediated by the Z boson. It is enhanced by the stronger $\tilde{\chi}_1^0$–$\tilde{\chi}_1^0$–Z coupling with increasing ε.

Fig. 4 summarizes all of our findings of the light Higgsino-LSP scenario in the BMSSM. For the MSSM parameters, we have chosen moderate values which can explain the WMAP data: $\mu = 120$ GeV, $\tan\beta = 3$, and $M_1 = 500$ GeV. We show, as functions of the parameter ε, the relic density $\Omega_{\tilde{H}}h^2$ in units of 0.1, the lightest Higgs boson mass m_h, the LSP mass $m_{\tilde{\chi}_1^0}$, the $\tilde{\chi}_1^\pm$ mass (all masses in units of 100 GeV), the Higgsino fraction $P_{\tilde{H}}$ of the LSP, and the spin-independent scattering cross section $\sigma_{\chi p}^{\rm SI}$ in units of 10^{-44} cm^2. As ε increases, the Higgs mass m_h increases but both $m_{\tilde{\chi}_1^0}$ and $m_{\tilde{\chi}_1^\pm}$ decrease. However, the mass difference $\Delta m_\pm$ increases while the Higgsino fraction $P_{\tilde{H}}$ of the LSP stays high $\sim$ 98%. We see a dramatic enhancement of the Higgsino-LSP relic density $\Omega_{\tilde{H}}h^2$ near $\varepsilon = 0.08$ or larger, where $\tilde{\chi}_1^0\tilde{\chi}_1^0 \to W^+W^-$ channel is kinematically closed. For our parameter choice, the light Higgsino-LSP of its mass about 82 GeV, when $\varepsilon \approx 0.085$, can explain all the observed CDM relic density in the Universe. For other choices of parameters we can still accommodate a light Higgsino-LSP as a primary candidate for the CDM relic density observed by the WMAP unless $\tan\beta$ is large.

5. Conclusions

The fine-tuning of the lightest Higgs boson mass m_h in the MSSM motivates additional interactions beyond the MSSM around the TeV scale. We have checked that, in the effective Lagrangian approach, the least-suppressed dimension-5 operator $\lambda(\hat{H}_u\cdot\hat{H}_d)^2/M$ added to the MSSM superpotential can usually increase m_h sufficiently for a moderate $\tan\beta$ and it can significantly affect the light Higgsino-LSP scenario. It lifts up the mass degeneracy between the LSP and the lighter chargino and that between the LSP and the second-lightest neutralino as much as a few tens of GeV. As a result, it is expected to improve significantly the chance of detecting the decay products of charginos and neutralinos at the LHC. Another important impact is on the Higgsino-LSP dark matter. Since the mass splittings suppress the coannihilation processes, the WMAP narrow band for the CDM relic density can accommodate a light Higgsino-LSP particle of its mass around 100 GeV for rather small $\tan\beta$.

Acknowledgements

We would like to thank Manuel Drees for valuable comments. The work of KC was supported by the NSC of Taiwan (96-2628-M-

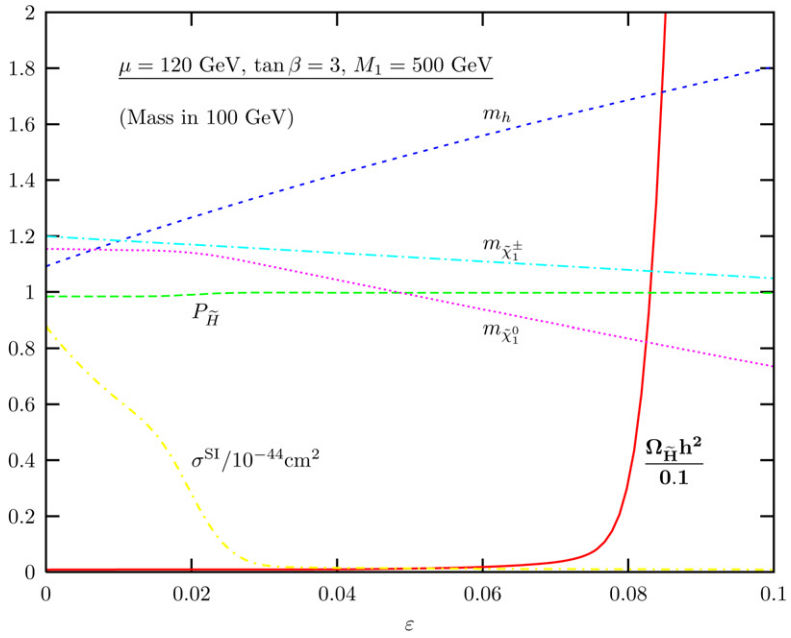

Fig. 4. As functions of ε, we present the relic density $\Omega_{\tilde{H}}h^2$ in units of 0.1, the lightest CP-even neutral Higgs boson mass m_h, the LSP mass, and the lighter chargino mass in units of 100 GeV, and the Higgsino fraction $P_{\tilde{H}}$ of the LSP. We fix $\mu = 120$ GeV, $\tan\beta = 3$, and $M_1 = 500$ GeV. Radiative corrections to the neutralino and chargino masses as well as to m_h are also included.

007-002-MY3), the Boost Project of NTHU, and the WCU program through the KOSEF funded by the MEST (R31-2008-000-10057-0). The work of S.Y.C. was supported by the KRF Grant funded by the Korean Government (KRF-2008-314-C00064). This work of J.S. was supported by the Konkuk University.

References

[1] D.N. Spergel, et al., WMAP Collaboration, Astrophys. J. Suppl. 170 (2007) 377, arXiv:astro-ph/0603449.
[2] G. Bertone, D. Hooper, J. Silk, Phys. Rep. 405 (2005) 279, arXiv:hep-ph/0404175.
[3] J.L. Feng, K.T. Matchev, T. Moroi, Phys. Rev. D 61 (2000) 075005, arXiv:hep-ph/9909334.
[4] K. Cheung, C.W. Chiang, J. Song, JHEP 0604 (2006) 047, arXiv:hep-ph/0512192.
[5] H.P. Nilles, Phys. Rep. 110 (1984) 1;
H.E. Haber, G.L. Kane, Phys. Rep. 117 (1985) 75.
[6] U. Chattopadhyay, D. Choudhury, M. Drees, P. Konar, D.P. Roy, Phys. Lett. B 632 (2006) 114, arXiv:hep-ph/0508098.
[7] M. Dine, N. Seiberg, S. Thomas, Phys. Rev. D 76 (2007) 095004, arXiv:0707.0005.
[8] A. Brignole, J.A. Casas, J.R. Espinosa, I. Navarro, Nucl. Phys. B 666 (2003) 105, arXiv:hep-ph/0301121.
[9] A. Strumia, Phys. Lett. B 466 (1999) 107, arXiv:hep-ph/9906266.
[10] H.P. Nilles, M. Srednicki, D. Wyler, Phys. Lett. B 120 (1983) 346;
J.M. Frere, D.R.T. Jones, S. Raby, Nucl. Phys. B 222 (1983) 11;
M. Drees, Int. J. Mod. Phys. A 4 (1989) 3635;
P.N. Pandita, Phys. Lett. B 318 (1993) 338;
S.F. King, P.L. White, Phys. Rev. D 52 (1995) 4183;
J.R. Espinosa, M. Quiros, Phys. Rev. Lett. 81 (1998) 516.
[11] J.A. Casas, J.R. Espinosa, I. Hidalgo, JHEP 0401 (2004) 008, arXiv:hep-ph/0310137.
[12] C.H. Chen, M. Drees, J.F. Gunion, Phys. Rev. D 55 (1997) 330, arXiv:hep-ph/9607421;
C.H. Chen, M. Drees, J.F. Gunion, Phys. Rev. D 60 (1999) 039901, Erratum.
[13] C. Amsler, et al., Particle Data Group, Phys. Lett. B 667 (2008) 1.
[14] J.R. Ellis, D.V. Nanopoulos, K.A. Olive, Phys. Lett. B 508 (2001) 65, arXiv:hep-ph/0102331.
[15] D. Pierce, A. Papadopoulos, Phys. Rev. D 50 (1994) 565, arXiv:hep-ph/9312248;
D.M. Pierce, J.A. Bagger, K.T. Matchev, R.j. Zhang, Nucl. Phys. B 491 (1997) 3, arXiv:hep-ph/9606211.
[16] G.F. Giudice, A. Pomarol, Phys. Lett. B 372 (1996) 253, arXiv:hep-ph/9512337.
[17] M. Drees, M.M. Nojiri, D.P. Roy, Y. Yamada, Phys. Rev. D 56 (1997) 276, arXiv:hep-ph/9701219;
M. Drees, M.M. Nojiri, D.P. Roy, Y. Yamada, Phys. Rev. D 64 (2001) 039901, Erratum.
[18] For a detailed discussion of the diagonalization of mass matrices, see the appendix of S.Y. Choi, H.E. Haber, J. Kalinowski, P.M. Zerwas, Nucl. Phys. B 778 (2007) 85, arXiv:hep-ph/0612218.
[19] J. Edsjo, P. Gondolo, Phys. Rev. D 56 (1997) 1879, arXiv:hep-ph/9704361.
[20] P. Gondolo, J. Edsjo, P. Ullio, L. Bergstrom, M. Schelke, E.A. Baltz, JCAP 0407 (2004) 008, arXiv:astro-ph/0406204.